Study of the D→Sb (D = O, S) Transannular Interaction in Sb-Monohalogenated Dibenzostibocines − An Experimental and Theoretical Study

José G. Alvarado-Rodríguez,*[a] Noemí Andrade-López,[a] Simplicio González-Montiel,[a] Gabriel Merino,[b] and Alberto Vela[b]

Keywords: Antimony / Density functional calculations / Halogens / Hypervalent compounds / Structure elucidation

In order to gain a greater insight in the nature of the D→Sb transannular interaction in dibenzostibocines, a series of $D(C_6H_4S)_2SbHal$ complexes (D = S; Hal = Cl **1**, Br **2**, I **3**; D = O, Hal = Cl **4**) has been synthesised. X-ray structure determinations of complexes **1**–**4** reveal that the antimony atom is in a distorted ψ-bipyramidal geometry, acting as an acceptor atom. The eight-membered ring conformation in **1**, **2** and **4** can be described as a twist-boat, while in **3** it is approaching C_s symmetry. DFT calculations were carried out on **1** and **4**. Topological analysis of the electron density in **1** and **4** showed the presence of critical points in the D→Sb direction (D = O, S). The electron localisation function showed the presence of a lone pair located in an equatorial position on the antimony, and a lone pair of the donor along the D→Sb direction, confirming the presence of a dative bond in the system.

Introduction

The coordinating capabilities of ligands such as **I** (unsubstituted or benzene ring-substituted) have been extensively studied, particularly in the formation of dibenzoheterocycles **II** (Scheme 1). These studies have focused mainly on the synthesis of heterodinuclear compounds containing nickel and iron for modelling of active sites of [NiFe] hydrogenases,[1,2] and also on structural investigations devoted to understanding of the factors involved in the valence expansion of the acceptor atom A through formation of intramolecular transannular bonds with D and its relation with the adopted conformation of the central eight-membered ring.[3,4]

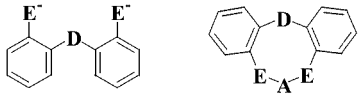

I **II**

A Lewis acid
D Lewis base
E O, S

Scheme 1

The coordination mode of **I** can mainly be di- or tridentate. In the first case, the lack of interactions results in atoms without valence expansion. The chemistry of the ligands with D = S and E = O is so far the most widely investigated. Metal complexes with *d*-block elements (Ti,[5] Zr,[6] V,[7] Co,[8] Cu,[9] W[10]) and light *p*-block elements, mainly phosphorus[11−13] and silicon,[4] acting as acceptor atoms A have been studied. Two spirocyclic germanium(IV) compounds containing ligands of type **I** (D = S, Se; E = O) have been crystallographically characterised. These compounds show the capabilities of **I** to expand the normal valence of the acceptor atom A.[14,15] In both cases, the germanium displays a distorted octahedral geometry with two transannular interactions D→Ge significantly shorter than the corresponding sums of the van der Waals radii.

For metal complexes **II** with D = S, and E = S, on the other hand, the chemistry is completely dominated by the *d*-block metals Fe,[16,17] Ni,[18−21] Pd[18−20] and Pt.[18,19] It is worth noting that, in the molecular structures determined in the solid state, the metal-sulfur (thioether) distance is always shorter than the metal-sulfur (thiolate) distance.

To the best of our knowledge, there are no reports of **II** complexes with heavier *p*-block elements, in particular complexes with antimony, in spite of the numerous studies carried out with similar stibocanes in which the presence of transannular D→A interactions and a large number of conformations of the eight-membered ring have been

[a] Centro de Investigaciones Químicas, Universidad Autónoma del Estado de Hidalgo,
Km. 4.5 Carretera Pachuca-Tulancingo, Pachuca, Hidalgo, México. C. P. 42076
Fax: (internat.) + 52-771/717-2000 ext. 6502
E-mail: galvarad@uaeh.reduaeh.mx
[b] Departamento de Química, Centro de Investigación y de Estudios Avanzados, I.P.N.
A. P. 14-740, México
Fax: (internat.) +52-55/5747-7113

  DOI: 10.1002/ejic.200300199

observed.[22−26] Here we report an experimental and theoretical study of type **II** complexes with antimony as acceptor atom. These compounds are good models for further understanding of the nature of the D→Sb interaction. After the description of the synthesis of stibocine Sb-halogen complexes, NMR and X-ray crystallographic data are presented and discussed. Finally, density functional theory (DFT) calculations on the chloro complexes are discussed, together with an analysis of the bonding based on some molecular scalar fields.

Results and Discussion

Synthesis of $D(C_6H_4S)_2SbHal$ (D = O, S; Hal = Cl, Br, I)

The $S(C_6H_4SH)_2$ compound was obtained in a four-step, one-pot reaction by the method reported by Sellmann.[19] The $O(C_6H_4SH)_2$ compound was obtained in a similar way (see Exp. Sect. for details). Treatment of $S(C_6H_4SH)_2$ and $O(C_6H_4SH)_2$ with $SbCl_3$ in benzene yielded $S(C_6H_4S)_2SbCl$ (**1**) and $O(C_6H_4S)_2SbCl$ (**4**), respectively (see Scheme 2).

1 D = S
4 D = O

Scheme 2

Both complexes are air-stable, soluble in benzene and chloroform, and insoluble in pentane, hexane and 2-propanol. $S(C_6H_4S)_2SbI$ (**3**) was obtained from a halogen-exchange reaction between **1** and two equivalents of KI in hot toluene, yielding pale-yellow crystals. However, $S(C_6H_4S)_2SbBr$ (**2**) could not be obtained in a similar way. More drastic conditions were tested, and compound **2** was synthesized from **1** by treatment with two equivalents of KBr in a refluxing HBr/toluene mixture, giving **2** as colourless crystals.

Mass Spectra

The FAB mass spectra of all the compounds each exhibit a low intensity ion with the appropriate isotopic ratio representing the molecular ion; in all cases the $M^+ - Hal$ peak is assigned to the $D(C_6H_4S)_2Sb$ tricyclic moiety, confirming the binding of antimony to sulfur atoms. No more peaks could be assigned.

NMR Spectroscopy

NMR spectroscopic data are given in Table 1. At 25 °C, the ^1H NMR spectra of **1** and **3** in $CDCl_3$ and the ^1H spectrum of **2** in C_6D_6 each show four signals in an ABCD pattern, typical of *ortho*-substituted benzene rings. In **4**, the ^1H NMR spectrum in $CDCl_3$ at the same temperature shows two signals at δ = 7.55 and 7.13 ppm for protons H-4 and H-2, respectively, and one more at δ = 7.18 ppm for H-1 and H-3 (see Scheme 3). In solution, the two C_6H_4S halves are equivalent. In all complexes, protons H-2 and H-4 are shifted to higher frequencies with respect to the free neutral ligand.

Table 1. ^1H NMR chemical shifts (δ values, ppm) for **1−4**

Compound	D	Hal	H-1	H-2	H-3	H-4
1[a]	S	Cl	7.51	7.27	7.16	7.60
2[b]	S	Br	7.01	6.61	6.54	7.21
3[a]	S	I	7.44	7.27	7.17	7.60
4[a]	O	Cl	7.18	7.13	7.18	7.55

[a] In $CDCl_3$. [b] In C_6D_6.

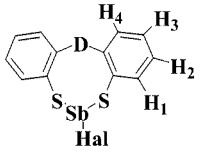

Scheme 3

The ^{13}C spectra of **1** and **3** in $CDCl_3$ at 25 °C each show the *ipso* carbons 1a (see Table 2, Scheme 4) at higher frequencies and the *ipso* carbons 4a at lower frequencies. An interesting observation in **3** is that the *ipso* carbon 1a is the most strongly shifted to lower frequencies. In **4**, the ^{13}C NMR spectrum in $CDCl_3$ at the same temperature shows C-1a and C-3 at 127.4 ppm; an APT experiment confirmed the previous result. The unequivocal assignment in **1** and **4** were performed by HETCOR and HMBC experiments.

Table 2. ^{13}C NMR chemical shifts (δ values, ppm) for **1−4**

Compound	D	Hal	C-1	C-1a	C-2	C-3	C-4	C-4a
1[a]	S	Cl	134.3	143.2	130.1	127.2	132.6	132.0
2[b]	S	Br	134.1	143.6	129.5	126.4	132.3	132.4
3[a]	S	I	134.8	141.9	129.9	127.2	132.2	132.1
4[a]	O	Cl	126.4	127.4	120.7	127.4	133.3	153.4

[a] In $CDCl_3$. [b] In C_6D_6.

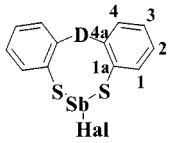

Scheme 4

The ^1H and ^{13}C NMR spectra of **1** in $CDCl_3$ at −65 °C show only a very small displacement to higher frequencies (less than 0.1 and 0.5 ppm in ^1H and ^{13}C NMR, respectively), showing that any conformational equilibrium is too fast to be determined.

X-ray Structures of Compounds 1−4

The solid-state structures of **1**−**4** were determined by single-crystal X-ray diffraction analyses. The structures are depicted in Figure 1. The unit cell of **3** has two crystallographically independent molecules (**3a** and **3b**). Compounds **1** and **2** co-crystallised with benzene and toluene, respectively. Selected bond lengths and angles are given in Table 3.

If the covalent bonds are taken into consideration, the structure determination of all complexes reveals tricoordinate pyramidal antimony atoms. The Sb−S distances are in good agreement with those reported in other eight-membered heterocycles containing antimony-sulfur bonds.[22−26] The Sb−Hal distances (Hal = Cl, Br, I) are 1−5% longer than the corresponding sums of the covalent radii [Σ_{rcov} (Sb,Cl) = 2.39 Å; Σ_{rcov} (Sb,Br) = 2.54 Å; Σ_{rcov} (Sb,I) = 2.73 Å][27,28] and compare well with other distances found in similar eight-membered heterocycles. In addition to the expected bonding of the two sulfurs (thiolate) and the halogen ligands to the antimony atom, a short distance of the transannular D atoms to Sb is observed (D = S in **1**, **2** and **3**; D = O in **4**). These distances are longer than the corresponding sums of covalent radii but shorter than the sums of the corresponding van der Waals radii, and can be described as secondary interactions.[29] Moreover, the S···Sb distance in the complexes **1**−**3** decreases in the order of *trans* substituents, with the shortest distance in the iodo complex **3**.

If the secondary interactions are taken into account, the geometry of the coordination sphere of the antimony atom can be described as ψ-trigonal bipyramidal (TBP), in which the halogen and thioether-like sulfur atoms are in the axial positions, the two thiolate-like sulfur atoms occupy two equatorial positions and, in terms of the VSEPR model, we are tempted to envisage a stereochemical activity of the lone pair of the antimony(III) atom in the fifth position. Furthermore, the degree of TBP coordination can be determined by

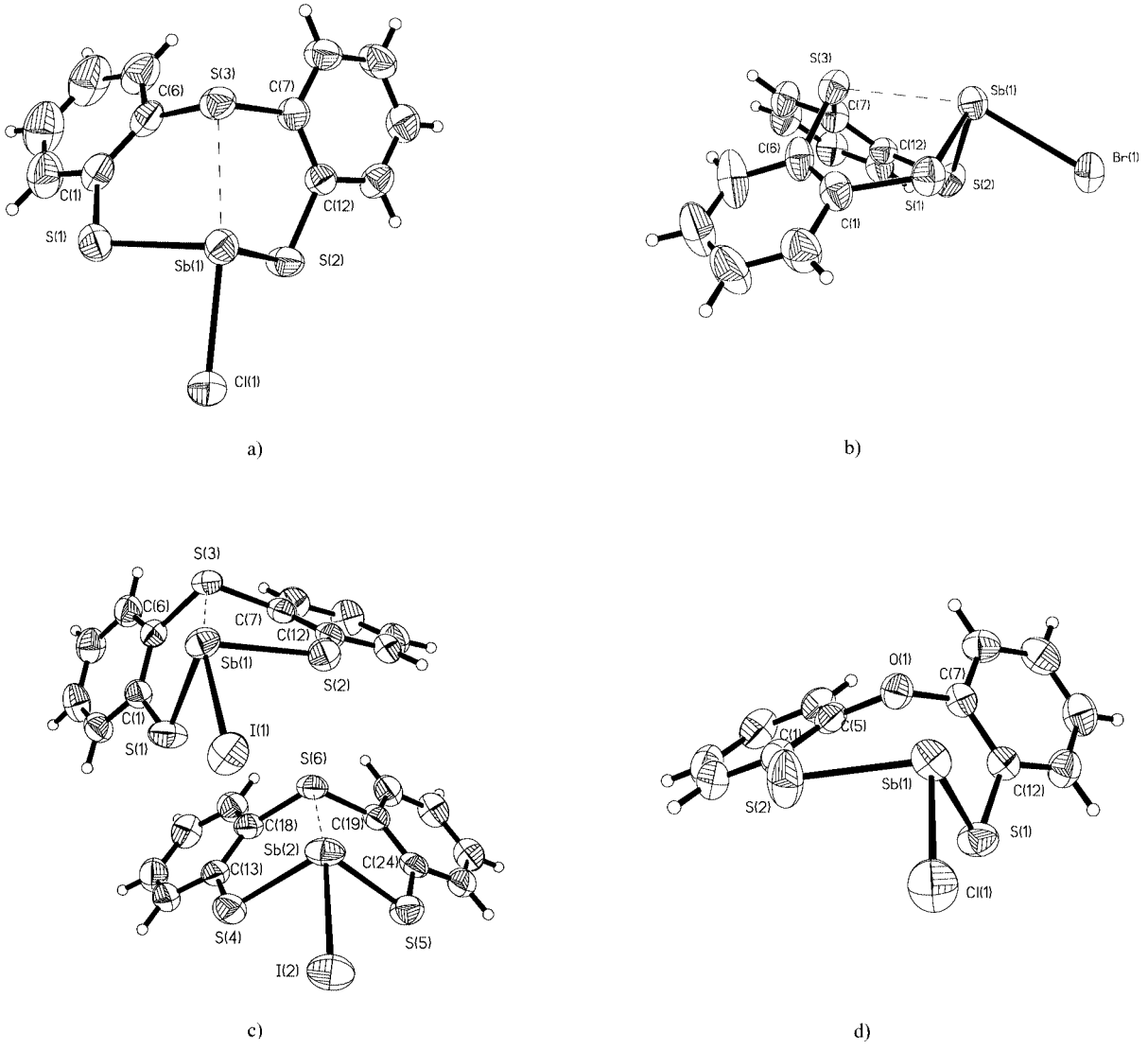

Figure 1. ORTEP diagrams of: a) $S(C_6H_4S)_2SbCl{\cdot}0.5C_6H_6$ (**1**·$0.5C_6H_6$), b) $S(C_6H_4S)_2SbBr{\cdot}0.5C_6H_5CH_3$ (**2**·$0.5C_6H_5CH_3$), and c) $S(C_6H_4S)_2SbI$ (**3**) and $O(C_6H_4S)_2SbCl$ (**4**) (50% probability ellipsoids, solvent molecules omitted)

Table 3. Selected bond lengths [Å] and bond angles [°] of $D(C_6H_4S)_2SbHal$

Compound	**1**·0.5C_6H_6	**2**·0.5$C_6H_5CH_3$	**3a**	**3b**	**4**
D	S	S	S	S	O
Hal	Cl	Br	I	I	Cl
Sb−Hal	2.4807(6)	2.6373(6)	2.8603(6)	2.8747(6)	2.4066(9)
Sb···D	2.8187(6)	2.8047(13)	2.7839(15)	2.7710(16)	2.596(2)
Sb−S(1)	2.4569(6)	2.4575(14)	2.4602(17)	–	2.4295(9)
Sb−S(2)	2.4640(6)	2.4637(14)	2.4445(15)	–	2.4280(10)
Sb−S(4)	–	–	–	2.4585(18)	–
Sb−S(5)	–	–	–	2.4639(17)	–
Hal−Sb···D	155.24(2)	155.86(4)	158.62(4)	158.61(4)	153.22(5)
S(1)−Sb−S(2)	98.39(2)	98.66(5)	95.71(6)	–	100.15(4)
S(4)−Sb−S(5)	–	–	–	96.38(6)	–
C(6)−D−C(7)	103.33(11)	103.3(3)	103.1(3)	–	116.2(2)
C(18)−D−C(19)	–	–	–	103.7(3)	–
C(1)−C(6)−D−C(7)	121.4(2)	122.5(5)	82.4(5)	–	139.6(3)
C(12)−C(7)−D−(C6)	−84.3(2)	−84.9(5)	−119.2(5)	–	−91.9(3)
C(1)−S(1)−Sb(1)−S(2)	−57.9(2)	−61.4(2)	−103.0(2)	–	−51.9(1)
C(12)−S(2)−Sb(1)−S(1)	104.3(8)	102.8(2)	65.8(2)	–	106.9(1)
C(13)−C(18)−D−C(19)	–	–	–	107.4(5)	–
C(24)−C(19)−D−C(18)	–	–	–	−98.4(5)	–
C(13)−S(4)−Sb(2)−S(5)	–	–	–	−80.5(2)	–
C(24)−S(5)−Sb(2)−S(4)	–	–	–	90.4(2)	–

a method used to describe structural displacements between pyramidal and trigonal bipyramidal idealised geometries.[30−32] In this method the degree of displacement from a lower (pyramidal) toward higher coordination geometry (TBP) is simply evaluated from the acceptor-donor atom distance and by how far this distance is displaced from the sum of the van der Waals radii (0% displacement) to the sum of covalent radii (100% displacement) of the acceptor-donor atoms. The results are presented in Table 4.

Table 4. Comparison of D···Sb−Hal geometrical bond parameters in **1−4** complexes; bond lengths in Å and bond angles in degrees

Compound	D	Hal	Sb···D	% TBP	D···Sb−Hal
1	S	Cl	2.8187(6)	73	155.24(2)
2	S	Br	2.8047(13)	74	155.86(4)
3a	S	I	2.7839(15)	76	158.62(4)
3b	S	I	2.7710(16)	77	158.61(4)
4	O	Cl	2.5960(2)	69	153.22(5)

The eight-membered ring conformations of compounds **1**, **2** and **4** can be described as twist-boat (C_1 symmetry).[15] This description is based on the non-equivalence of the torsional angles, mainly those formed by the torsion of the carbon-sulfur (thioether) bond and the antimony-sulfur (thiolate) bond (Table 3). The ring conformation of compound **3** deserves some comments. In the **3a** molecule the conformation can also be described as twist-boat, but in **3b** the conformation could better described as boat-boat (C_s symmetry). This proposal is supported by the closer similitude between the torsion angles of the C−C−D−C and C−S−Sb−S atoms (ca. 10°).

DFT Calculation on Compounds 1 and 4

In order to analyse the bonding situation in the different molecules we performed a set of DFT calculations. The systems were fully optimised, and the nature of the chemical bonding was analysed in terms of the topology of the electronic density [$\rho(\mathbf{r})$[33]] and the electron localisation function [ELF($\mathbf{r}$)[34,35]].

All calculations were performed with the aid of Gaussian 98,[36] by use of the hybrid functional BHandHLYP. The selection of this hybrid functional was made for one reason. The half-and-half mixing of exact exchange and density-dependent exchange is justified by approximating the adiabatic connection formula.[37] For the geometry optimization, the 6-31++G(d,p) basis set was employed for all atoms, except for the antimony, for which a relativistic effective core potential (RECP) was used.[38] We denote these calculations as BHandHLYP/6-31++G(d,p) + RECP(Sb). All stationary points were characterised on the potential energy surface by a harmonic frequency analysis. For the generation of the molecular scalar fields, a double-ζ basis set with one polarisation function in all atoms (DZVP) was used.[39] The contractions of the DZVP basis set are (41/1*) for hydrogen, (621/41/1*) for carbon and oxygen, (6321/521/1*) for sulfur and chlorine, and (633321/53321/531*) for antimony. These calculations are denoted as BHandHLYP/DZVP. The Kohn−Shan orbitals were determined by BHandHLYP/DZVP//BHandHLYP/6-31++G(d,p) + RECP(Sb). The analysis of the electron density and the ELF were performed with the aid of the AIM2000[40] and the TopMod[41] programs, respectively.

A set of selected bond lengths and angles of the optimised structures are reported in Table 5. The calculated geometrical parameters are in good agreement with the crystallographic data. In relation to the initial structure in

Table 5. Selected experimentally measured and theoretical bond lengths and bond angles of $D(C_6H_4S)_2SbCl$ (D = S, O); bond lengths are in Å and bond angles are in degrees; dipole moments are in Debyes

	1[a]	**1**[b]	**1′**[b]	**4**[a]	**4**[b]	**4′**[b]
Sb−Cl	2.4807(6)	2.415	2.425	2.4066(9)	2.393	2.394
Sb···D	2.8187(6)	3.002	2.902	2.596(2)	2.697	2.614
Sb−S(1)	2.4569(6)	2.469	2.463	2.4295(9)	2.455	2.446
Sb−S(2)	2.4640(6)	2.460	–	2.4280(10)	2.461	–
S(1)−C(1)	1.773(2)	1.776	1.772	1.766(3)	1.772	1.773
S(2)−C(12)	1.771(2)	1.776	–	1.769(3)	1.777	–
C(6)−D	1.791(3)	1.786	1.787	1.412(4)	1.388	1.393
C(7)−D	1.790(2)	1.781	–	1.414(3)	1.385	–
Cl−Sb···D	155.24(2)	158.8	160.7	153.22(5)	155.4	156.9
Cl−Sb−S(1)	85.66(2)	93.2	88.1	90.09(3)	93.3	90.3
Cl−Sb−S(2)	84.38(2)	91.1	–	88.64(3)	94.4	–
C(1)−S(1)−Sb	107.39(9)	104.9	109.5	104.30(11)	104.0	102.6
C(12)−S(2)−Sb	105.28(7)	102.8	–	97.00(10)	95.9	–
C(6)−D−Sb	99.46(8)	94.4	100.4	113.04(16)	111.5	113.1
C(7)−D−Sb	98.63(8)	93.0	–	104.58(16)	102.0	–
D···Sb−S(1)	79.32(2)	73.7	79.5	72.88(5)	71.7	74.7
D···Sb−S(2)	78.538(18)	75.2	–	74.69(5)	70.7	–
S(1)−Sb−S(2)	98.39(2)	99.5	99.6	100.15(4)	101.6	97.3
C(6)−D−C(7)	103.33(11)	103.2	105.4	116.2(2)	117.9	123.9
Dipole	–	6.27	7.1	–	5.87	6.45

[a] Experimental data. [b] Theoretical data.

the solid, the largest deviations are found in the D→Sb (D = O, S) and Sb−Cl bonds. The Sb−D bond length in the solid state is shorter than calculated for the gas phase. This behaviour is very common in donor-acceptor molecules and it is a consequence of the electrostatic dipole-dipole interactions (μ = 6.27 and 5.87 D in **1** and **4**, respectively).[42,43]

Of the possible isomers, the C_s structures (denoted as **1′** and **4′**, respectively) were considered, and their geometrical parameters are summarised in Table 5. These structures are transition states on the corresponding potential energy surface. Harmonic analysis shows one small imaginary frequency (−33 and −52 cm^{-1} in **1′** and **4′**, respectively). The relative energies of isomers **1′** and **4′** with respect to the unsymmetrical structures are ΔE = 3.2 and 4.2 kcal/mol, respectively. On the other hand, the Sb···D distances are smaller in the C_s structures than in unsymmetrical isomers. The largest bond length difference between the C_s and C_1 structures is the Sb···D distance (≈0.1 Å in **1** and ≈0.08 Å in **4**). It is worth noting that the Sb···D distances in the C_s structures are closer to the solid-state data and they have the largest dipole moment. This is in line with the model suggesting that donor-acceptor complex systems are stabilized by the dipole-dipole interactions.

To analyse the bonding in molecules **1** and **4**, the critical points of the electron density (CPs) and the gradient paths were determined. Here we focus the analysis mainly on the (3,-1) saddle points. Results of topological analysis of the electron density (TAED) are presented in Table 6, and the molecular graphs of **1** and **4** are depicted in Figure 2. All systems show bond critical points along the Sb···D directions, even though these distances are longer than the Sb−S(1) and Sb−S(2) bond lengths. The values of ρ_c(D···Sb) are smallest (≈0.027 a.u.) and $\nabla^2\rho_c$ are positive.

Table 6. Topological analysis of the electronic density; ρ, L and ε are the density, Laplacian ($-1/4\nabla^2\rho$) and ellipticity at the critical points, respectively; all quantities are in atomic units

	D = S			D = O		
	ρ	L	ε	ρ	L	ε
Sb−Cl	0.074	−0.032	0.027	0.077	−0.034	0.029
Sb···D	0.029	−0.014	0.053	0.026	−0.022	0.113
Sb−S(1)	0.079	−0.015	0.134	0.081	−0.015	0.162
Sb−S(2)	0.079	−0.015	0.139	0.080	−0.015	0.146
S(1)−C(1)	0.192	0.089	0.119	0.192	0.090	0.132
S(2)−C(12)	0.192	0.090	0.120	0.192	0.089	0.110
C(6)−D	0.192	0.090	0.099	0.260	0.061	0.019
C(7)−D	0.194	0.092	0.077	0.263	0.064	0.034

It is important to note that the L values of all bond critical points connecting Sb with its neighbours are negative, three interactions are stronger than the dative bond and have a very important ionic contribution.

The distribution of the lone pairs in the complexes is therefore a crucial question. In this sense, the electron localisation function is a good molecular scalar field with which to study this situation. The local maxima of this function define attractors corresponding to core, bonding and non-bonding electron pairs. The analysis of the ELF for molecules **1** and **4** are presented in Figure 3. The first important feature to note is the presence of a lone pair located on the antimony atom. At the same time, there are two basins around the equatorial sulfur atoms, which are related to the lone pairs on these atoms. However, the situation of the possible donor atom is special. In this case, the D atom has two basins, but one of them is found along the D→Sb interaction. On the other hand, one of lone pairs of the D atom is oriented towards antimony.

Figure 2. Molecular graphs of **1** and **4**; the small black and light grey spheres are the bond and ring critical points, respectively

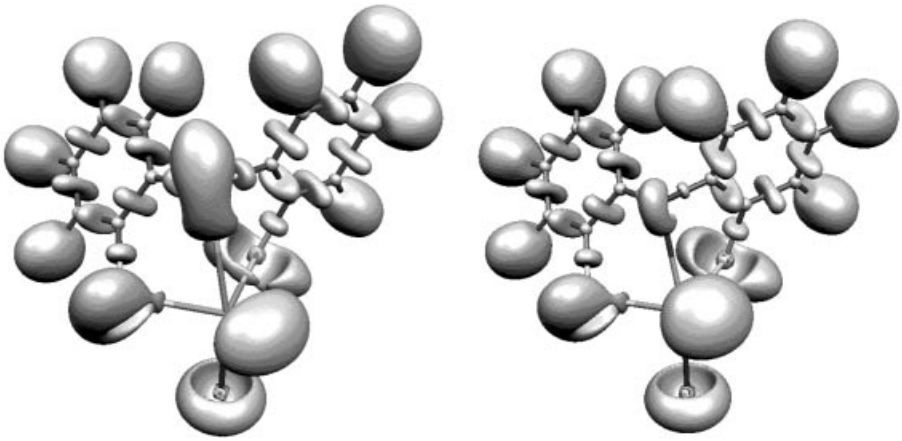

Figure 3. ELF isosurfaces [ELF(**r**) = 0.85] for **1** and **4**

The analyses presented above allow us to classify these molecules as intramolecular donor-acceptor complexes, in which Sb acts as an acceptor and the D atom as a donor.

Concluding Discussion

In the quest for good models with which to understand the nature of the D→Sb interactions, the complexes $D(C_6H_4S)_2SbHal$ **1**−**4** have been synthesised, structurally characterised and theoretically studied. All compounds display a distorted ψ-bipyramidal trigonal geometry of the antimony atom.

The X-ray analysis of the transannular Sb···S distances in the complexes **1**−**3** are 16.5−4.5% longer than the corresponding sums of the covalent radii and they indicate secondary bonding. This situation is different from that in *d*-block metals complexes in which the metal-sulfur (thioether) distance is shorter than the metal-sulfur (thiolate) distance. The Sb···S distance decreases as the electronegativity of the halogen ligand decreases. Moreover, there is a correlation between the symmetry of the eight-membered ring and the transannular distance: the higher the symmetry of the ring, the shorter the Sb···S distance, reflecting the flexibility of the $[S(C_6H_4S)_2]^{2-}$ ligand. In the chloro stibocine derivatives, the sulfur atom is a better donor that the oxygen atom. This is also consistent with the larger % TBP displacement determined in **1**.

The theoretical calculations predict a Sb···D bond length longer than in the solid state. This is a typical effect when a donor-acceptor complex is formed. On the other hand, the relative energies of the symmetrical isomers (**1′** and **4′**) with respect to unsymmetrical structures are ΔE = 3.2 and 4.2 kcal/mol, respectively, in agreement with the NMR results in which the conformational equilibria are too fast to be determined. Molecules **1** and **4** show bond critical points along the Sb···D directions. The topological descriptors allow us to classify the Sb···S interaction as a weak interaction. The ELF for the molecules **1** and **4** indicates the presence of a lone pair located on the antimony atom at the equatorial position. The D atoms (D = S, O in **1** and **4**, respectively) have two basins, one of them being found

along the D→Sb direction. These experimental and theoretical results allow us to classify these compounds as intramolecular donor-acceptor complexes in which the antimony atom acts as acceptor atom.

Experimental Section

General Methods: Unless noted otherwise, all reactions and operations were carried out under argon at room temperature with use of standard Schlenk techniques. Solvents were dried and distilled before use. Melting points were determined on a Melt-Temp II instrument and are uncorrected. Spectra were recorded with the following instruments. Mass spectra: for EI, a Hewlett Packard 5989A mass spectrometer was used. FAB+ mass spectra were recorded on a JEOL JMS-AX505HA by using a Xe beam at 6 keV, with nitrobenzyl alcohol (NBA) as matrix. Elemental analysis: Perkin-Elmer Series II CHNS/O Analyzer. The IR spectra were record in the 4000−400 cm^{-1} range on a Perkin−Elmer System 2000 FT-IR spectrometer, as KBr pellets or in CsI cuvettes. NMR: Jeol Eclipse 400 spectrometer; with the residual protio-solvent signal used as referenced for ^1H NMR spectra. $^{13}C\{^1H\}$ NMR spectra were referred through the solvent peaks. Chemical shifts are quoted on the δ scale (downfield shifts are positive) relative to tetramethylsilane (^1H, $^{13}C\{^1H\}$). Spectra were recorded at 25 °C. ^1H; 399.78 MHz, $^{13}C\{^1H\}$; 100.53 MHz. $S(C_6H_5)_2$, $O(C_6H_5)_2$, *n*BuLi (1.6 M, in hexanes), KI, KBr and HBr were purchased from Aldrich and Fluka. $SbCl_3$ was sublimed prior to use. The $S(C_6H_4SH)_2$ compound was prepared as reported.[19]

$O(C_6H_4SH)_2$: TMEDA (12.20 mL, 81.15 mmol), a solution of *n*BuLi in hexanes (1.6 M, 50 mL, 80 mmol) and diphenyl ether (6 mL, 37.85 mmol) were successively added at room temperature to 60 mL of hexanes. The solution was stirred for 24 h, in the course of which a beige solid precipitated. Elemental sulfur (3.46 g, 108.00 mmol) was added with vigorous stirring, and the resulting yellow suspension was stirred for 48 h and concentrated to dryness. The yellow residue was dissolved in THF (60 mL) and immersed in an ice bath, and $LiAlH_4$ (3.02 g, 84.85 mmol) was added in small portions. ***Caution: A vigorous reaction takes place and the reaction suspension starts to foam.*** Subsequently, the reddish-brown suspension was heated at reflux for 5 h, in the course of which the colour turned to light yellow green. The resulting mixture was cautiously added in small portions to a mixture of crushed ice (60 g) and concentrated hydrochloric acid (60 mL) immersed in an ice-bath. ***Caution: Vigorous evolution of H_2 and H_2S occurs, and this reaction must be carried out in a well ventilated fumehood.*** After the vigorous reaction had ceased, further concentrated hydrochloric acid (20 mL) was added, and the resulting suspension was extracted with CH_2Cl_2 (3 × 60 mL). The combined organic phases were washed with dilute HCl and passed through a column of Celite and Na_2SO_4, and evaporation of the solvent yielded a yellow oil. Yield: 3.0 g (34%) $O(C_6H_4SH)_2$. MS (EI, CH_2Cl_2): *m*/*z* = 234 [$M^{\cdot+}$ peak base], 200 [$M^{\cdot+}$ − H_2S]. ^1H NMR ($CDCl_3$): δ = 3.90 (s, 2 H, SH), 6.82 (dd, 2 H, C_6H_4), 7.04 (dt, 2 H, C_6H_4), 7.09 (dt, H, C_6H_4), 7.36 (dd, 2 H, C_6H_4) ppm. $^{13}C\{^1H\}$ NMR ($CDCl_3$): δ = 118.6, 123.7, 124.5, 126.7, 130.2, 152.1 ppm. IR (CsI): $\tilde{\nu}$ = 3052, 2555 (SH), 1582, 1446, 1426, 1036, 747 cm^{-1}. The neutral ligand was used further without purification.

$S(C_6H_4S)_2SbCl$ (1): A solution of freshly sublimed $SbCl_3$ (1.62 g, 7.10 mmol) in benzene (25 mL) was added dropwise to a solution of $S(C_6H_6SH)_2$ (1.76 g, 7.03 mmol) in benzene (25 mL). The yellow solution was stirred for 30 min, upon which a green solution resulted, and this was heated at reflux for 5 h. The solution was allowed to cool to room temperature. The resulting colourless crystals of **1**, as a benzene solvate, were separated by suction filtration and washed with *i*PrOH (40 mL). Yield: 2.40 g (84%) based on $S(C_6H_4S)_2SbCl$ free compound. FAB+: *m*/*z* (%) = 404 (4) [$M^{\cdot+}$], 369 (17) [$M^{\cdot+}$ − Cl]. M.p. 183−189 °C. $S(C_6H_4S)_2SbCl{\cdot}0.5C_6H_6$ (444.66): calcd. C 40.52, H 2.49; found C 39.29, H 2.36. ^1H NMR ($CDCl_3$): δ = 7.16 (ddd, 2 H, C_6H_4), 7.27 (ddd, 2 H, C_6H_4), 7.51 (dd, 2 H, C_6H_4), 7.60 (dd, 2 H, C_6H_4) ppm. $^{13}C\{^1H\}$ NMR ($CDCl_3$): δ = 127.17, 130.1, 132.0, 132.6, 134.3, 143.2 ppm. IR (KBr): $\tilde{\nu}$ = 3048, 1568, 1444, 1421, 1035, 744 cm^{-1}.

$S(C_6H_4S)_2SbBr$ (2): $S(C_6H_4S)_2SbCl{\cdot}0.5C_6H_6$·(**1**·$0.5C_6H_6$, 160 mg, 0.36 mmol), KBr (86 mg, 0.72 mmol) and HBr 48% (2 mL) were suspended in toluene (25 mL) and heated at reflux for 16 h. The water was removed from the resulting colourless solution by means of a Dean−Stark trap. The yellow solution obtained was dried by passage through a column of Celite and Na_2SO_4. The solution was left under an argon flow to provide yellow crystals of **2** as a toluene solvate, which were washed with hexanes (40 mL) and filtered by suction. Yield: 100 mg (62% based on free compound **2**). FAB+: *m*/*z* (%) = 448 (5) $[M]^+$, 369 (74) $[M - Br]^+$. M.p. 193−194 °C. $S(C_6H_4S)_2SbBr\ 0.5C_6H_5CH_3$ (496.13): calcd. C 37.52, H 2.44; found C 37.61, H 2.26. ^1H NMR (C_6D_6): δ = 6.54 (td, 2 H, C_6H_4), 6.62 (td, 2 H, C_6H_4), 7.01 (dd, 2 H, C_6H_4), 7.21 (dd, 2 H, C_6H_4) ppm. $^{13}C\{^1H\}$ NMR (C_6D_6): δ = 126.4, 129.5, 132.3, 132.4, 134.1, 143.6 ppm. IR (KBr): $\tilde{\nu}$ = 3046, 1568, 1443, 1420, 1245, 1036, 745 cm^{-1}.

$S(C_6H_4S)_2SbI$ (3): $S(C_6H_4S)_2SbCl\ 0.5C_6H_6$·(**1**·$0.5C_6H_6$, 160 mg, 0.36 mmol) and KI (120 mg, 0.72 mmol) were suspended in dry toluene (25 mL) and heated at reflux for 16 h. The yellow solution was dried by passage through a column of Celite and Na_2SO_4 whilst still warm, and was then allowed to cool to room temperature. On cooling, yellow crystals separated, and these were washed with *n*-hexanes (40 mL) and filtered by suction. Yield: 71 mg (40%). FAB+: *m*/*z* (%) = 496 (2) $[M]^+$, 369 (5) $[M - I]^+$. m.p. 200−204 °C. $S(C_6H_4S)_2SbI$ (497.05): calcd. C 29.00, H 1.62; found C 28.98, H 1.55. ^1H NMR ($CDCl_3$): δ = 7.17 (ddd, 2 H, C_6H_4), 7.27 (ddd, 2 H, C_6H_4), 7.44 (dd, 2 H, C_6H_4), 7.60 (dd, 2 H, C_6H_4) ppm. $^{13}C\{^1H\}$ NMR ($CDCl_3$): δ = 127.2, 129.9, 132.1, 132.2, 134.8, 141.9 ppm. IR (KBr): $\tilde{\nu}$ = 3045, 1569, 1447, 1415, 1247, 1034, 742 cm^{-1}.

$O(C_6H_4S)_2SbCl$ (4): A solution of $O(C_6H_6SH)_2$ (2.0 g, 8.54 mmol) in benzene (25 mL) was added to a solution of $SbCl_3$ (1.95 g, 8.54 mmol) in benzene (25 mL). The yellow solution was stirred for 30 min and was heated to reflux for 5 h. The solution was allowed to cool to room temperature. On cooling, colourless crystals separated, and these were washed with *i*PrOH (40 mL) and filtered by suction. Yield: 1.76 g (53%). FAB+: *m*/*z* (%) = 388 (2) $[M]^+$, 353 (5) $[M - Cl]^+$. m.p. 164−5 °C. $O(C_6H_4S)_2SbCl$ (389.54): calcd. C 37.00, H 2.07; found C 36.65. H 2.12. ^1H NMR ($CDCl_3$): δ = 7.11−7.20 (m, 6 H, C_6H_4), 7.53−7.58 m, 2 H, C_6H_4) ppm. $^{13}C\{^1H\}$ NMR ($CDCl_3$): δ = 120.7, 126.4, 127.4, 133.3, 153.41 ppm. IR (KBr): $\tilde{\nu}$ = 3055, 1584, 1458, 1435, 1054, 752 cm^{-1}.

X-ray Structure Analysis of $S(C_6H_4S)_2SbCl{\cdot}0.5C_6H_6$ (1·0.5C_6H_6), $S(C_6H_4S)_2SbBr{\cdot}0.5CH_3C_6H_5$ (2·0.5 $CH_3C_6H_5$), $S(C_6H_4S)_2SbI$ (3) and $O(C_6H_4S)_2SbCl$ (4)

Suitable single crystals of **1** were grown by slow evaporation of the solvent from a benzene solution, and crystals of **2** and **3** were grown similarly from toluene solutions. Single crystals of **4** were grown by slow diffusion of pentane into a **4**/toluene solution in a 5:1 solvent ratio

Table 7. Selected crystallographic data for complexes **1**−**4**

Compound	**1**	**2**	**3**	**4**
Empirical formula	$C_{15}H_{11}ClS_3Sb$	$C_{15.53}H_{12}BrS_3Sb$	$C_{12}H_8IS_3Sb$	$C_{12}H_8ClOS_2Sb$
M_r [g/mol]	444.62	496.50	497.01	389.50
Crystal size [mm]	0.50 × 0.21 × 0.10	0.13 × 0.19 × 0.20	0.15 × 0.23 × 0.25	0.08 × 0.10 × 0.28
F(000)	1736	1914	928	752
Crystal system	Monoclinic	Monoclinic	Triclinic	Monoclinic
Space group	$C2/c$	$C2/c$	$P\bar{1}$	$P2_1/c$
a (Å)	23.3503(9)	23.4224(9)	9.3319(6)	4.6860(3)
b (Å)	8.1526(3)	8.3738(3)	11.6186(7)	15.6037(10)
c (Å)	18.3156(8)	18.3659(7)	13.8542(9)	17.8196(10)
α [°]	90	90	103.0640(10)	90
β [°]	109.525(1)	110.193(1)	92.518(2)	91.303(2)
γ [°]	90	90	104.584(2)	90
V (Å^3)	3286.2(2)	3380.8(2)	1407.97(15)	1302.61(14)
Z	8	8	4	4
$\rho_{calcd.}$ [Mg/m^3]	1.797	1.951	2.345	1.986
μ [mm^{-1}]	2.209	4.355	4.571	2.622
Temperature [K]	293(2)	293(2)	294(2)	294(2)
θ range [°]	1.85 to 26.52	1.85 to 26.00	1.52 to 26.00	1.73 to 26.57
Reflections collected	10991	10884	9554	9004
Unique. reflections	3420	3328	5514	2713
R_{int}	0.0358	0.0614	0.0516	0.0605
Solution method	Direct	Patterson	Patterson	Direct
$R1$; $wR2$ [$I > 2\sigma(I)$]	0.0248, 0.0588	0.0342, 0.0830	0.0352, 0.0778	0.0287, 0.0518
$R1$; $wR2$ [all data]	0.0291, 0.0610	0.0501, 0.1003	0.0548, 0.0900	0.0431, 0.0560
Largest residuals [e·Å^{-3}]	0.472/−0.560	0.709/−0.932	0.752/−1.270	0.432/−0.765

Suitable crystals were glued and mounted on fibre glass with the aid of epoxy resin. Intensity data were collected at room temperature on a CCD Smart 6000 diffractometer through the use of Mo-K_α radiation (λ = 0.71073 Å, graphite monochromator). Empirical absorption correction was applied for all complexes. The structures were solved by direct (**1**, **4**) or heavy atom (**2**, **3**) methods, and full-matrix, least-squares refinement was carried out on F^2 (SHELXTL NT 5.10).[44] All non-hydrogen atoms were refined anisotropically. The positions of the hydrogen atoms were kept fixed with a common isotropic displacement parameter. Selected crystallographic data are given in Table 7.[45]

Acknowledgments

JGAR gratefully acknowledges the CONACyT (Project J27919-E) for financial support for these investigations. We wish to thank Dra. Verónica García Montalvo (UNAM) for the recording of FAB+ Mass Spectra.

[1] D. Sellmann, F. Geipel, F. W. Heinemann, *Chem. Eur. J.* **2002**, *8*, 958.
[2] D. Sellmann, F. Geipel, F. Laudebach, F. W. Heinemann, *Angew. Chem. Int. Ed.* **2002**, *41*, 632.
[3] A. J. Arduengo, C. A. Stewart, *Chem. Rev.* **1994**, *94*, 1215−1237.
[4] R. R. Holmes, *Chem. Rev.* **1996**, *96*, 927−950, and references therein cited.
[5] F. Amor, S. Fokken, T. Kleinhenn, T. P. Spaniol, J. Okuda, *J. Organomet. Chem.* **2001**, *621*, 3−9.
[6] L. Porri, A. Ripa, P. Colombo, E. Miano, S. Capelli, S. V Meille, *J. Organomet. Chem.* **1996**, *514*, 213−217.
[7] C. R. Cornman, K.M. Geiser-Bush, J. W. Kampf, *Inorg. Chem.* **1999**, *38*, 4303.
[8] H. Muller, A. Holzmann, W. Hinrichs, G. Klar, *Z. Naturforsch., Teil B* **1982**, *37*, 341.
[9] P. Chaudhuri, M. Hess, U. Florke, K. Wieghardt, *Angew. Chem. Int. Ed.* **1998**, *37*, 2217.
[10] Y. Nakayama, H. Saito, N. Ueyama, A. Nakamura, *Organometallics* **1999**, *18*, 3149.
[11] R. R. Holmes, *Acc. Chem. Res.* **1998**, *31*, 535−542, and references therein cited.
[12] R. R. Holmes, A. Chandrasekaran, P. Sood, R. O. Day, *Inorg. Chem.* **1999**, *38*, 3369−3376.
[13] R. R. Holmes, A. Chandrasekaran, R. O. Day, P. Sood, N. V. Timosheva, D. J. Sherlock, *Phosphorus, Sulfur and Silicon* **2000**, *160*, 1−27.
[14] S. D. Pastor, V. Huang, D. Nabi-Rahni, S. A. Koch, H.-F. Hsu, *Inorg. Chem.* **1997**, *36*, 5966.
[15] T. Thompson, S. D.Pastor, G.Rihs, *Inorg. Chem.* **1999**, *38*, 4163.
[16] D. Sellmann, F. Geipel, F. W. Heinemann, *Chemistry A European Journal* **2002**, *8*, 958.
[17] D. Sellmann, F. Geipel, F. Lauderbach, F. W. Heinemann, *Angew. Chem. Int. Ed.* **2002**, *41*, 632.
[18] D. Sellmann, F. Geipel, F. W. Heinemann, *Eur. J. Inorg. Chem.* **2000**, 59.
[19] D. Sellmann, D. Haussinger, *Eur. J. Inorg. Chem.* **1999**, 1715.
[20] D. Sellmann, F. Geipel, F. W. Heinemann, *Eur. J. Inorg. Chem.* **2000**, 4279.
[21] D. Sellmann, F. Geipel, F. W. Heinemann, *Eur. J. Inorg. Chem.* **2000**, 271.
[22] M. Draeger, R. Engler, *Z. Anorg. Allg. Chem.* **1974**, *405*, 183−192.
[23] M. Draeger, *Z. Anorg. Allg. Chem.* **1976**, *424*, 183−189.
[24] H. M. Hoffmann, M. Draeger, *J. Organomet. Chem.* **1985**, *295*, 33−46.
[25] H. M. Hoffmann, M. Draeger, *J. Organomet. Chem.* **1987**, *320*, 273−281.
[26] M. A. Muñoz Hernández, R. Cea Olivares, S. Hernández Ortega, *Z. Anorg. Allg. Chem.* **1996**, *622*, 1392−1398.
[27] r_{cov}(Sb) = 1.40, r_{cov} (O) = 0.73, r_{cov} (S) = 1.02, r_{cov} (Cl) = 0.99, r_{cov} (Br) = 1.14, r_{cov} (I) = 1.33, = 1.40, r_{vdW} (O) = 1.52,

r_{vdw} (S) = 1.80, r_{vdW} (Cl) = 1.75, r_{vdW} (Br) = 1.85, r_{vdw} (I) = 1.96 Å, from W. W. Porterfield, *Inorganic Chemistry: A Unified Approach*, 2nd ed., Academic Press, Inc. USA **1993**, p. 214.
[28] r_{vdW} (Sb) = 2.12 Å, in A. Bondi, *J. Phys. Chem.* **1964**, *68*, 441−451.
[29] N. W. Alcock, *Adv. Inorg. Chem. Radiochem.* **1972**, *15*, 1−50.
[30] A. Chandrasekaran, P. Sood, R. O. Day, R. R. Holmes, *Inorg. Chem.* **1999**, *38*, 3369−3376.
[31] N. V. Timosheva, A. Chandrasekaran, R. O. Day, R. R. Holmes, *Inorg. Chem.* **1998**, *37*, 3862−3867.
[32] D. J. Sherlock, A. Chandrasekaran, R. O. Day, R. R. Holmes, *Inorg. Chem.* **1997**, *36*, 5082−5089.
[33] R. F. Bader, *Atoms in Molecules: A Quantum Theory*; Oxford University Press: Oxford, U. K., **1994**.
[34] A. D. Becke, K. E. Edgecombe, *J. Chem. Phys.* **1990**, *92*, 5397−5403.
[35] B. Silvi, A. Savin, *Nature* **1994**, *371*, 683−686.
[36] *Gaussian 98, Revision A.7*, M. J. Frisch, G. W. Trucks, H. B. Schlegel, G. E. Scuseria, M. A. Obb, J. R. Cheeseman, V. G. Zakrzewski, J. A. Montgomery, Jr., R. E. Stratmann, J. C. Burant, S. Dapprich, J. M. Millam, A. D. Daniels, K. N. Kudin, M. C. Strain, O. Farkas, J. Tomasi, V. Barone, M. Cossi, R. Cammi, B. Mennucci, C. Pomelli, C. Adamo, S. Clifford, J. Ochterski, G. A. Petersson, P. Y. Ayala, Q. Cui, K. Morokuma, D. K. Malick, A. D. Rabuck, K. Raghavachari, J. B. Foresman, J. Cioslowski, J. V. Ortiz, A. G. Baboul, B. B. Stefanov, G. Liu, A. Liashenko, P. Piskorz, I. Komaromi, R. Gomperts, R. L. Martin, D. J. Fox, T. Keith, M. A. Al-Laham, C. Y. Peng, A. Nanayakkara, M. Challacombe, P. M. W. Gill, B. Johnson, W. Chen, M. W. Wong, J. L. Andres, C. Gonzalez, M. Head-Gordon, E. S. Replogle, J. A. Pople, Gaussian, Inc., Pittsburgh, PA, **1998**.
[37] J. Harris, *Phys. Rev.* **1984**, *A29*, 1648−1659.
[38] C. E. Check, T. O. Faust, J. M. Bailey, B. J. Wright, T. M. Gilbert, L. S. Sunderlin, *J. Phys. Chem. A* **2001**, *105*, 8111−8116.
[39] N. Godbout, D. R. Salahub, J. Andzelm, E. Wimmer, *Can. J. Chem.* **1992**, *70*, 560−571.
[40] *AIM2000*, version 1.0, Biegler-Köning, University of Applied Sciences, Bielefeld, Germany, **2000**.
[41] *ToPMoD package*, S. Noury, X. Krokidis, F. Fuster, B. Silvi, B.; Universite Pierre et Marie Curie, Paris, France, **1997**.
[42] G. Merino, V. I. Bakhmutov, A. Vela, *J. Phys. Chem.* **2002**, *106*, 8491−8494.
[43] A. Haaland, *Angew. Chem. Int. Ed. Engl.* **1989**, *28*, 992−1007.
[44] *SHELXTL 5.10 Bruker AXS*, Inc., Madison, WI, USA 1998.
[45] CCDC-207115 (**1**·0.5C_6H_6), -207117 (**2**·$C_6H_5CH_3$), -207118 (**3**) and -207116 (**4**) contain the supplementary crystallographic data for this paper. These data can be obtained free of charge at www.ccdc.cam.ac.uk/conts/retrieving.html [or from the Cambridge Crystallographic Data Centre, 12, Union Road, Cambridge CB2 1EZ, UK; Fax: (internat.) + 44-1223/336-033; E-mail: deposit@ccdc.cam.ac.uk].

Received April 8, 2003
Early View Article
Published Online August 14, 2003

